PAPER REFERENCE NUMBER: PM290

SESSION REFERENCE NUMBER: WO3.4

HOPPING TRANSPORT IN n-a-Si:H EMITTERS OF SILICON HETEROSTRUCTURE SOLAR CELLS

C. Boehme, J. Behrends, K. v. Maydell,
M. Schmidt and K. Lips

Hahn-Meitner-Institut Berlin,

Kekuléstr. 5, D-12489 Berlin

Germany

Word count:

Title, one affiliation, 123 word abstract:	623	journal page words
6 manuscript pages of text	1517	journal page words
5 section titles at 25 words each	125	journal page words
9 References at 15 words each	135	journal page words
4 single column figures at 150 words each	600	journal page words
	3000	journal page words

3000 words /750 words per page = 4 pages

HOPPING TRANSPORT IN n-a-Si:H EMITTERS OF SILICON HETEROSTRUCTURE SOLAR CELLS

C. Boehme, J. Behrends, K. v. Maydell, M. Schmidt, and K. Lips

Hahn-Meitner-Institut Berlin, Kekuléstr. 5, D-12489 Berlin, Germany

Abstract

Hopping transport through heterostructure solar cells based on B-doped crystalline silicon wafers with highly P-doped hydrogenated amorphous silicon emitters with different thicknesses is investigated at T = 10 K with pulsed electrically detected magnetic resonance. The measurements show that transport is dominated by conduction band tail states ($g \approx 2.0046$) with a distribution of their mutual coupling strength. The signal intensity correlates to the sample thickness and the g-factors do not exhibit an anisotropy which suggests that transport is still dominated by bulk properties of amorphous silicon. In addition, two broad P-donor hyperfine satellites can be detected. Influences of interface defects such as P_b-like states known from silicon dioxide interfaces are either suppressed by the high Fermi-energy at the interface or not present.

PACS:

72.20.Ee Mobility edges; hopping transport

72.25.Dc Spin polarized transport in semiconductors

72.20.Jv Charge carriers: generation, recombination, lifetime, and trapping

76.90.+d Other topics in magnetic resonances and relaxations

1. Introduction

Heterostructure solar cells based on B-doped crystalline silicon (c-Si) wafers with highly P-doped hydrogenated amorphous silicon (n-a-Si:H) emitters are manufactured without high temperature processes which has made them increasingly attractive for technological applications in recent years. In spite of this, the physics of the c-Si/n-a-Si:H interface at the heart of these devices still lacks of an understanding with regard to the electronic processes thereat (transport, recombination). It is unknown whether the electronic processes are dominated by either the bulk properties of the thin n-a-Si:H layer or the c-Si interface properties or whether a new comprehensive description of this heterostructure is necessary. The band structure of the n-a-Si:H/c-Si heterojunction as known from simulation studies [1] and UV excited photoemission studies [2] is sketched in fig.1. With the indicated Fermi energy, it is conceivable that spin-dependent charge carrier hopping through conduction band tail states and phosphorous donor states can take place at low temperatures. When n-a-Si:H bulk properties are dominant, one would anticipate that charge carrier transport is influenced by conduction band tail states as well as the phosphorous donors while recombination could be influenced by randomly oriented n-a-Si:H silicon dangling bonds. When interface properties dominate, P_b-like states known from the c-Si/SiO_2 interface could be involved in electronic transitions [3].

In the following, a low temperature (T= 10K) pulsed electrically detected magnetic resonance (pEDMR) study on photocurrents through the n-a-Si:H/c-Si interfaces is presented whose aim was to identify the electronic transitions thereat.

2. Experiments

PEDMR is based on the transient measurement of coherent electron spin resonance (ESR) induced changes of spin-dependent electronic transitions that influence macroscopic conductivities. Similar to the traditional continuous wave (cw) EDMR which is a well established defect spectroscopy method [4], pEDMR is very sensitive (it can detect the spin motion of only a few hundred spins), yet, unlike cw EDMR, pEDMR allows to observe coherent spin propagation which makes it possible to attain information about coupling strength and coherence times and therefore transition probabilities for the electronic processes investigated [5,6].

Figure 1 (inset) displays a schematic sketch of the test structures which were used for the experiments presented here: The samples consist of a (100) surface oriented, slightly B-doped c-Si substrate which is covered with 200nm thick thermally grown silicon dioxide layer where a window area of $1mm^2$ was etched out in order to accommodate the thin (between 2.4 nm and 20nm) P-doped n-a-Si:H layer underneath an 80nm thick, transparent, conducting, and highly n-doped ZnO layer. The sample was contacted on the back with a less than 200nm thin Al layer and at the front with a 100µm wide and less than 200nm thick Al grid. For the pEDMR experiment, the sample was cooled down to T=10K and exposed continuously to a 100W halogen lamp which, when focused onto the sample surface caused a homogeneous irradiation with cold light (UV and IR components were filtered) of approximately $100mW/cm^2$. In order to establish vertical charge transport through the sample, a negative bias of 0.7V was applied such that a negative steady state current was established. The pulsed ESR excitation during application of a constant magnetic field (B_0) was carried out by a Bruker E580 spectrometer at X-Band around a frequency of 9.7GHz. The inset of fig. 2 displays the photocurrent (PC) change from the steady state value after a pulse excitation of

the g=2.0046 resonance with τ=160ns length and 32W intensity. Note that on the given µs-time scale, the pulse excitation is instantaneous. Thus, the current transient reflects the gradual return of the spin-ensemble to its steady state. It can be shown [5] that the integration Q of this current relaxation which represents the charges transported due to the sudden change of the spin-ensemble is proportional to its singlet content. Hence, the measurement of Q is the coherent spin-measurement of the electronic states in resonance at the end of the pulse and consequently, by measuring $Q(\tau)$ as a function of the pulse length τ, one can observe the coherent propagation of the excited defect on a ns-time scale whereas the measurement of $Q(B_0)$ as a function of externally applied constant magnetic field B_0 for a fixed pulse length reveals the Landé factors and line shapes of the paramagnetic states that influence conductivity.

3. Results

Figure 2 displays the B_0-dependence of Q on a logarithmic scale. Note that Q was measured by integration of the current between $0<\tau<200$µs. The current transient measured during this time is plotted in the inset for the magnetic field value corresponding to g=2.0046. The fit of the $Q(B_0)$ data with two Gaussian and one Lorentzian line shape (solid line) reveals the presence of two Gaussian ESR contributions with similar intensity, an identical peak width of 7.8mT and a separation of 23mT. In addition, the Lorentzian line reveals a much stronger and much more narrow peak (1.8mT) at g=2.0046(2). Measurements at samples with different n-a-Si:H layer thicknesses showed no qualitative change of the observed $Q(B_0)$ spectra but a increase of the signal intensity with the used layer thickness (not shown here).

In order to prove that the observable Q represents the coherent spin-state of the respective resonance at the end of the 160ns long pulses, a pulse lengths dependence $Q(\tau)$ was measured for different applied microwave field strength at g=2.0046 as displayed in fig. 3. As one can see, $Q(\tau)$ has an oscillatory behavior similar to the theoretical predictions for electrically detected Rabi oscillation [5] whose frequency $\Omega = \sqrt{\gamma B_1 + (\omega_L - \omega)^2}$ is predicted to be proportional to B_1 (γ is a proportionality factor which depends on coupling within the spin pair as well as the gyromagnetic ratio [5]) when resonance conditions are established ($\omega = \omega_L$). The B_1-field dependence $\Omega(B_1)$ of the Rabi frequency was extracted from the different $Q(\tau)$ measurements (with a fast Fourier transform, [FFT]) and displayed versus the B_1-field as shown in the inset of fig. 3: As one can infer from the excellent agreement of the data and the linear fit through the origin, the oscillation is clearly due to Rabi oscillation. Note that the scaling of the absolute B_1-fields was obtained from the power broadening of $Q(B_0)$ measurements similar to those of fig. 2 (not shown here).

4. Discussion and conclusions

The measurements displayed in fig. 2 show that transport through the n-a-Si:H/c-Si hetero interface exhibits the same spin-dependent signatures than plain n-a-Si:H films [7,8]. Since (i) no contributions of P_b like states or other anisotropic contributions from the c-Si interfaces [9] were recognizable, and (ii) the intensities of the signals correlate to the n-a-Si:H thickness, we conclude that n-a-Si:H bulk properties determine the interface transport.

Figure 4 displays a FFT of the electrically detected spin-Rabi oscillation during a microwave pulse with B_1=0.5mT which is displayed in fig. 3. One can clearly see three different peaks 1

to 3 whose center frequencies, widths and intensities are displayed in the inset table. Thus, the resonantly excited electronic transition at g=2.0046, namely the electron hopping through conduction band tail states in n-a-Si:H, is not one sharply defined process which is homogeneous throughout the material but a rather complex group of qualitatively different transitions. Note that the intensities of the peaks 1 to 3 decrease with increasing center frequencies whereas at the same time, the peak widths increase. Within the margin of the fit errors, the center frequency Ω_1 of peak 1 is just half the center frequency Ω_3 of peak 3. Hence, with the pEDMR theory described elsewhere [5] it becomes obvious that pairs of conduction band states can exist with a variety of coupling strength which are illustrated for the qualitatively distinguishable regimes in the table of fig. 4:

Peak 1 in fig.4 is associated with transitions between weakly coupled pairs with two $s=1/2$ spin systems since the Larmor separation $\Delta\omega=\mu_B B_0(g_a-g_b)$ within the pair must be larger than the exchange coupling J and the microwave field B_1. Obviously, these transitions are very homogeneous and thus, we conclude that they are due to transitions between band tail states with large spatial separation, high localization and different local environments which may be due to slightly different electronic energies. Peak 2 is due to strong exchange coupled pairs ($J>B_1$, $\Delta\omega$) with little spatial separation, and little inhomogeneity. We conclude that this channel is representative of transitions between states with stronger delocalization and therefore larger wave function overlap. Peak 3 is due to a Larmor separation and exchanges coupling smaller than the microwave field $B_1>\Delta\omega, J$ that can have either strong exchange coupling of states with overlapping wave functions or weak exchange coupling between states with similar g-factors. It is conceivable that there can be a continuous range of spatial localizations and spatial separations between states which fall into this category. We conclude that this continuous range is reflected by the inhomogeneity of peak 3.

5. Summary

The investigation of hopping transport through n-a-Si:H/c-Si hetero interfaces showed that the excess charge transport at T=10K is dominated by known n-a-Si:H bulk states, even when film thicknesses as little as 24Å are present. For the hopping transitions through conduction band tail states, the electrical detection of spin-Rabi oscillation was demonstrated. From this data, it could be concluded that a variety of different coupling situations between the electronic states where transitions occur, exist.

References

[1] R. Stangl, A. Froitzheim, in Proc. of the 18th European PV Conf. (Rome, Italy, 2002), 123.

[2] M. Schmidt et al., in Proc of the 19th European PV Conf. (Paris, France, 2004), 592.

[3] R. Müller, P. Kanschat, S. von Aichberger, K. Lips, W. Fuhs; *J. of Non-Cryst. Solids* **266-269** (2000), 1124.

[4] M. Stutzmann, M. S. Brandt, and M.W. Bayerl, J. Non–Cryst. Solids **266-269**, 1 (2000).

[5] C. Boehme and K. Lips, Phys. Rev. B **68**, 245105 (2003).

[6] C. Boehme and K. Lips, Phys. Rev. Lett **91**, 24, 246603 (2003).

[7] K. Lips, S. Schütte, and W. Fuhs, Phil. Mag. B **65**, 945 (1992).

[8] M. S. Brandt and M. Stutzmann, Appl. Phys. Lett. **58**, 1620 (1991).

[9] P. M. Lenahan and J. F. Conley, J. Vac. Sci. Technol. B **16**, 2134 (1998).

Figure Caption Sheet

PAPER REFERENCE NUMBER: PM290

SESSION REFERENCE NUMBER: WO3.4

HOPPING TRANSPORT IN n-a-Si:H EMITTERS OF SILICON HETEROSTRUCTURE SOLAR CELLS

C. Boehme, J. Behrends, K. v. Maydell, M. Schmidt, and K. Lips

Fig. 1:

Sketch of the band diagram of the n-a-Si:H/c-Si heterostructure as well as the different localized defect states involved based on a simulation presented elsewhere [1]. Inset: Cross sectional sketch of the test structure for the n-a-Si:H/c-Si interface.

Fig. 2:

The magnetic field dependence of the integrated current change Q (Which is defined to be the integrated PC between $t = 0$ and $t = 200\mu s$ as indicated in the inset) plotted on a logarithmic scale. The fit (solid lines) reveals the influence of a strong Lorentzian shaped resonance at $g = 2.0046(4)$ and the two smaller Gaussian peaks with similar widths and intensities at $g = 2.076(2)$ and $g = 1.942(2)$, respectively. Inset: Transient of the spin-dependent PC (ΔI represents the difference of the current from its steady state value) through the n-a-Si:H/c-Si heterointerface at $T = 10$ K right after a coherent microwave excitation of the $g = 2.0046$ resonance.

Fig. 3:

Electrically detected Rabi oscillation during a coherent microwave excitation measured for different microwave fields B_1 at the g = 2.0046 resonance. Inset: The main frequency component of the Rabi oscillation displayed in the main plot as a function of the microwave field strength B_1. A fit with a linear function (solid line through the origin) reveals an excellent agreement.

Fig. 4:

Fast Fourier transform (FFT) of the electrically detected Rabi oscillation during a coherent microwave excitation as displayed in fig. 3 for B_1 = 0.5 mT. The data is fit with three Lorentzian peaks (solid line) whose fit results for centers frequencies, line width and intensities are displayed in the inset table along with sketches of coupling situations associated with these Rabi frequencies.

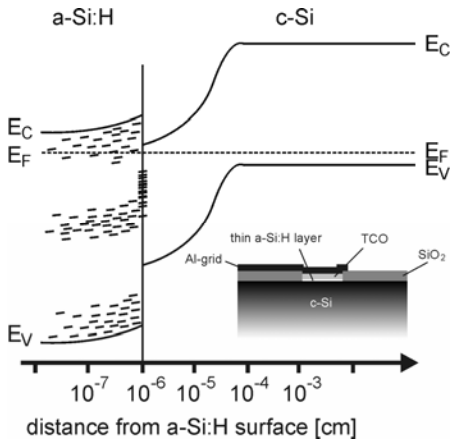

Boehme et al., ref. - #: PM290, session-ref. - # WO3.4, Fig. 1

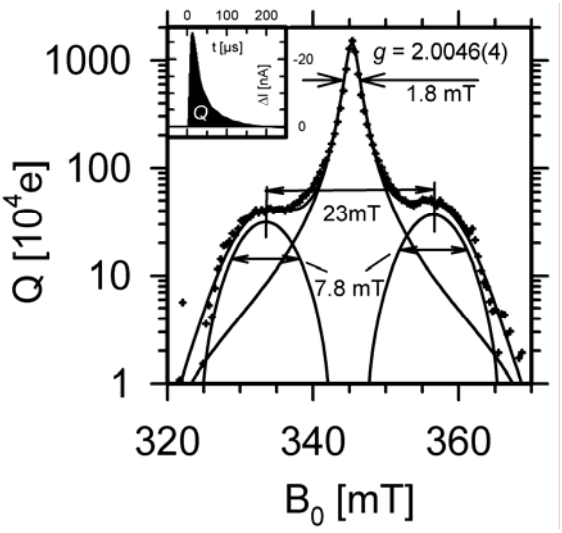

Boehme et al., ref. - #: PM290, session-ref. - # WO3.4, Fig. 2

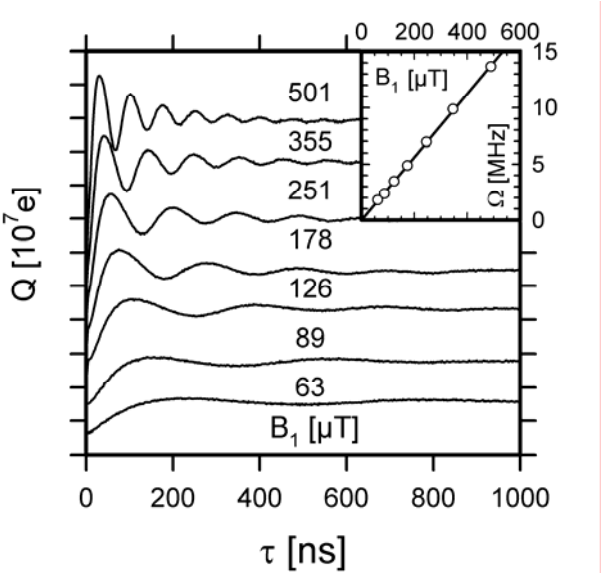

Boehme et al., ref. - #: PM290, session-ref. - # WO3.4, Fig. 3

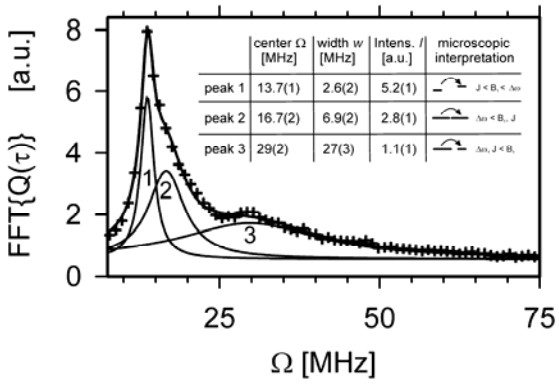

Boehme et al., ref. - #: PM290, session-ref. - # WO3.4, Fig. 4